J. Nig. Ass. Math. Phys
Vol. 3 (1999)

UNIFIED HAMILTONIAN MODEL FOR MAGNETISM AND SUPERCONDCTIVITY IN HIGH -T_C CUPRATE SYSTEMS

G.C. ASOMBA
DEPARTMENT OF PHYSICS AND ASTRONOMY
UNIVERSITY OF NIGERIA, NSUKKA, NIGERIA
AND
A.O.E. ANIMALU
NATIONAL MATHEMATICAL CENTRE, ABUJA, NIGERIA

ABSTRACT

A mean-field Hamiltonian model, applicable to the high-T_C cuprate oxide systems, is represented, under the name: pairing t-model (PtM), which unifies some known Hamiltonian models for strong electron correlation (usually leading to magnetism) and the popular Bardeen - Cooper - Schrieffer (BCS) model for electron pairing (leading to superconductivity). The PtM emphasizes electron kinetics as, perhaps, the most important operative factor in the high-T_C cuprates. The analysis is based on a 4 × 4 matrix Green's function method using the generalised pseudospin matrices of the type: $A_{\rho\lambda} = \Lambda_\rho \otimes \Lambda_\lambda$ ($\rho,\lambda = 0,1,2,3...$ where $\Lambda_{\rho(\lambda)}$ are dummies for the Pauli (σ_ρ), Dirac ($\alpha_\rho,\beta,\gamma_\rho,\Sigma_\rho$), Gell-Mann ($\alpha_\rho$), .. matrices) first introduced in the mapping of the novel pairing scheme in the multiple-band cuprates, by one of us, and some of the $\sigma_\rho \otimes \sigma_\lambda$ components recently used in the hadronic mechanics (Lie-isotopic) treatment of the Cooper pair by one of us. Some of the new results obtained for the normal and superconducting excitation energies, superconducting energy gap, transition temperature and density of states, for the cuprates, have similarities with the corresponding results from experiment and the recent interlayer Josephson tunneling model by Anderson but may have advantages over the latter.

1 INTRODUCTION

In the new copper oxide (cuprate) superconducting (SC) materials, a number of not-so-well understood features complicate the direct application of the popular Hubbard, t-J, or Bardeen-Cooper-Schrieffer (BCS)[1] models of electron (hole) correlation and pairing. These features include: (i) electron hopping, (ii) energy multi-band structure, (iii) band overlap and hybridization, (iv) normal state antiferromagnetism (AF), (v) charge transfer (CT), (vi) strong lattice distortions (tetragonal ↔ orthorhombic (Jahn-Teller (JT) effect)), (vii) molecular (planar?) Cu(2) 3d - O(2,3) 2p conductivity, (viii) oxygen doping effect, (ix) copper ion valence fluctuation, (x) level symmetry shifts, (xi) coupled electron-lattice (vibronic) motion, and (xii) high SC critical temperature (T_c). On account of the above multiplicity of novel features, if the standard (BCS) model of conventional

SC, on the basis of the impelling advantages of its rich understanding, has to be promoted to achieve dominating relevance to high-T_c systems, it must be extended and/or reinterpreted. Accordingly, this has been done in a number of recent papers[2-8] under the names 'isostandard BCS model'[14] and mean-field (MF) 'pairing t-model' (PtM)[7,8].

In its simplest non-relativistic form, the isostandard model[4] of SC is a generalisation of the Lurie - Cremer[9] quasiparticle wave equation,

$$i\frac{\partial}{\partial t}\Psi(r,t) = H\Psi(r,t), \qquad H = \frac{1}{2m_t}p^2\tau_3 + \Delta\tau_1, \tag{1.1}$$

via an isotopic lifting of the underlying "metric" (g),

$$g \equiv \tau_3 = \begin{pmatrix} 1 & 0 \\ 0 & -1 \end{pmatrix} \rightarrow \tau_3 = \begin{pmatrix} 1 & 0 \\ 0 & -T \end{pmatrix} \equiv g, \tag{1.2}$$

which is characterised by a nonlocal integral operator (T). The later is defined by

$$T\psi^*_{\downarrow}(r) = \int dr' [\delta(r-r') - \psi^*_{\uparrow}(r)\psi_{\uparrow}(r')]\psi^*_{\downarrow}(r') \tag{1.3}$$

where $\psi^*_{\uparrow}(r)$ and $\psi^*_{\downarrow}(r)$ are the two spinor components of the quasiparticle wave function $\psi(r,0)$ in the Nambu representation; $P^2/2m$ is the kinetic energy operator (measured from the Fermi level, E_F); and Δ is the electron pairing energy. It is apparent from (1.3) that when the overlap integral or "orthogonalisation" term:

$$Z^{1/2} = \int dr'\psi^*_{\downarrow}(r')\psi^*_{\uparrow}(r') \equiv \langle\psi^*_{\downarrow}|\psi^*_{\uparrow}\rangle \tag{1.4}$$

vanishes, T reduces to unity and we recover the standard model exactly. Note that we may rewrite T in the form

$$T = 1 - |\psi_{\uparrow}\rangle\langle\psi^*_{\uparrow}|, \tag{1.5}$$

so that $T^2 = T$ if $\langle\psi^*_{\uparrow}|\psi_{\uparrow}\rangle = 1$. This shows that T is an idempotent (projection) operator.

Similarly, the MF pairing t - model[7,8] is based on an equivalent generalisation of the standard hopping Hamiltonian in the second - quantized form

$$H = -\sum_{ijk\sigma} t_{ijk}\hat{C}^+_{ik\sigma}\hat{C}_{jk\sigma}, \tag{1.6}$$

where the operator corresponding to T in (1.5) is defined by

$$\hat{C}^{+}_{ik\sigma} = T_{ik\sigma}C^{+}_{ik\sigma} \equiv (1 - n_{ik\sigma})\, C^{+}_{ik\sigma},\ n_{ik\sigma} = C^{+}_{ik\sigma}C_{ik\sigma}, \tag{1.7}$$

and similarly for $\hat{C}_{ik\sigma}$, where $\sigma = \uparrow$ for $\overline{\sigma} = \downarrow$, and vice versa. Here, i(j) = d, p labels electrons (bands) of Cu 3d and/or O 2p characters whose wavefunctions may overlap and/or bands hybridize; t_{ijk} (i(j) = 1, 2, ...,N) is the nearest-neighbour electron transfer (hopping) integral, and $C^{+}_{ik\sigma}$ ($C_{ik\sigma}$) is the fermion creation (annihilation) operator for i-electron with crystal vector k. By virtue of the transformation (1.7), only single occupancy per spin site is permitted but double occupancy of an orbital site is not forbidden. In this paper, we shall consider a minimum of two bands (N=2) of like or unlike characteristics, and this will involve a generalisation of the 2 x 2 Pauli pseudospins (σ_λ) to the 4 x 4 ($A_{\sigma\lambda}$, p, λ = 0,1, 2,3) Dirac-type pseudospins *introduced*[6] in the generalised[5-8] Nambu representation of electron pair states in multiple band pairing schemes.

2. THE PAIRING t-MODEL HAMILTONIAN FORMALISM

The extension of the standard BCS model, in this paper, is based on a consideration of electron kinetics, which is dependent on electron hopping in the constrained Hilbert space presented by the high-T_c cupates. As shown[8], the generalised hopping Hamiltonian (1.6) can be written approximately in the MF form:

$$H = \sum_{ik\sigma}\varepsilon_{ik\sigma}C^{+}_{ik\sigma}C_{ik\sigma} - \sum_{ijk\sigma, i\neq j} t_{ijk}C^{+}_{ik\sigma}C_{jk\sigma} + \sum_{ijk\sigma, i\neq j}(\Delta_{iik}C^{+}_{ik\sigma}C^{+}_{ik\sigma} + g_{iik}C^{+}_{ik\sigma}C^{+}_{jk\sigma} + \text{h.c.}), \tag{2.1}$$

where $\varepsilon_{ik\sigma}$, which is the Fourier transform of $t_{ii\sigma}$, is i-electron unperturbed kinetic energy relative to the Fermi level, E_F; the Hermitian energy gaps in i-band (i≠j):

$$\Delta_{iik} = t_{iik} < C_{ik\sigma}C_{ik\overline{\sigma}} > -\sum_{j} U_{ijk} < C_{ik\sigma}C_{jk\overline{\sigma}} >, \tag{2.2a}$$

$$g_{iik} = t_{iik} < C_{ik\sigma}C_{ik\overline{\sigma}} > -\sum_{j} U_{iik} < C_{ik\sigma}C_{jk\overline{\sigma}} >, \tag{2.2b}$$

correspond, respectively, to intraband-pair and hybrid-pair (Zhang and Rice (ZR) - pair)[10] conductivity, with

$$U_{ijk} = t_{ijk} < C_{ik\sigma}C_{jk\overline{\sigma}} >, \tag{2.3a}$$

$$U_{iik} = t_{ijk} < C_{ik\sigma}C_{ik\overline{\sigma}} >. \tag{2.3b}$$

$$U_{ijk} = t_{ijk} < C_{ik\sigma} C_{jk\bar{\sigma}} >, \quad (2.3a)$$

$$U_{iik} = t_{ijk} < C_{ik\sigma} C_{ik\bar{\sigma}} >. \quad (2.3b)$$

The structure of the gaps (2.2) is similar to that by Anderson[11] which was recently analysed by Chakravarty et al[12]. Eqn. (2.1) has the form of the standard BCS model[1] but now includes intraband and interband hopping and ZR-pairing. Observe that t_{iik} is now analogous to the pairing potential $V_{kk'}$ in the standard model[1] and U_{ijk} (U_{iik}) analogous to the interband pairing potential $V_{ijkk'}$ of the generalised model due to Suhl et al.[13] This analogy permits possible re-interpretation of the BCS model in terms of the electron hopping matrices.

The most useful form of the solutions of the PtM is in terms of the Nambu-Gor'kov Green's function at finite temperatures which has a general 4×4 matrix form:

$$G(k, i\omega_n) = uG_s(k, i\omega_n) + vG_a(k, i\omega_n), \quad (2.4)$$

in which the subscript s(a) refers to the symmetric (antisymmetric) spin energy regime, and the coefficients u and v which are functions of doping variables, are related by

$$u^2 + v^2 = 1. \quad (2.5)$$

In this sense, $v \approx 1$ for normal cuprates, and $u \approx 1$ for the doped systems, and the two constitute tunable parameters deserving further investigation. The time variable $\omega_n (n = 0, \pm 1, \pm 2 \ldots, \pm\infty)$ is the fermion Mutsubara frequency.

Further simplification is achieved by employing the spin energy antisymmentry condition[2,7,8] while specialising to two (d,p) bands, henceforth:

$$\varepsilon_{pk\sigma} = -\varepsilon_{dk\downarrow} = \varepsilon_{dk\uparrow} = -U/2; \quad \Delta_{ddk} = -\Delta_{ppk} = -t_{ijk}(i \neq j). \quad (2.6)$$

It yields the system's Green function as the inverse matrix

$$G_a(k, i\omega_n) = [i\omega_n - \xi_{ak}(A_{00} - A_{03}) - \alpha_{ak}A_{33} - \Delta_{ak}A_{13} + g_{ak}A_{22}]^{-1}, \quad (2.7)$$

$$\xi_{ak} = \tfrac{1}{4}((\varepsilon_{dk\uparrow} - \varepsilon_{dk\downarrow}) - (\varepsilon_{pk\downarrow} - \varepsilon_{pk\uparrow})), \quad (2.8a)$$

$$\alpha_{ak} + \alpha_{sk} = \tfrac{1}{4}((\varepsilon_{dk\uparrow} + \varepsilon_{dk\downarrow}) - (\varepsilon_{pk\uparrow} + \varepsilon_{pk\downarrow})) \quad (2.8b)$$

$$\Delta_{ak} = \tfrac{1}{2}(\Delta_{ddk} - \Delta_{ppk}), \quad (2.8c)$$

$$g_{ak} = \tfrac{1}{2}(g_{ddk} - g_{ppk}), \quad (2.8d)$$

This reveals[7,8] the antisymmetric-state AF and CT regimes of the normal cuprates. The conditions in Eqn. (2.6) insure double occupancy (complete filling) and single occupancy (half-filling), respectively, of O 2p and Cu 3d orbital sites

as exist in the cuprates. This, indeed, constitutes the very basic but important physics of the normal state cuprate.

In contrast, by employing the symmetric (equalisation) condition[7,8], which is also the generalised BCS criterion[6]

$$\varepsilon_{ik\sigma} = \varepsilon_k; \Delta_{iik} = \Delta_k, \tag{2.9}$$

the SC regime is revealed[7] with the system Green's function now given by

$$G_s(k, i\omega_n) = [i\omega_n - \theta_{sk}A_{30} - \alpha_{sk}A_{33} - \Delta_{sk}A_{10} + g_{sk}A_{11} + tA_{31}]^{-1}, \tag{2.11}$$

where

$$\theta_{sk} = (1/2N) \sum_{i\sigma} \varepsilon_{ik\sigma}, \tag{2.11}$$

and Δ_{sk} and g_{sk} are the symmetric conjugates of Δ_{ak} and g_{ak}, respectively, while regarding $t = t_{ij}$ $(i \neq j)$, as may arise. The parameter α_{sk} follows level symmetry shifts.

In (2.7) and (2.10), the matrices

$$A_{\rho\lambda} = \sigma_\rho \otimes \sigma_\lambda, \ (\rho,\lambda = 0,1,2,3) \tag{2.12}$$

have the significance as illustrated typically by

$$A_{31} = \sigma_3 \otimes \sigma_1 = \begin{pmatrix} 0 & \sigma_3 \\ \sigma_3 & 0 \end{pmatrix}, \tag{2.13}$$

where σ_ρ is the 2×2 Pauli spin matrix (for $\rho = 1,2,3$) and the unit matrix (for $\rho = 0$). The matrices (2.12) constitute the required generalisation[3,8] of the 4×4 α - and β -Dirac matrices first introduced in the contractive Nambu representation of electron-pair states in the cuprates, in the doctoral thesis[5], and subsequently employed in the recent hadronic mechanics treatment of the Cooper pair problem[3] and in some earlier works[14]. Notice that

$$\gamma_0 = A_{03}, \gamma_5 = A_{01}, \qquad \Gamma(\text{or } \Sigma) = \sigma \otimes \sigma_0 \tag{2.14}$$

are, respectively, the parity, chiral helicity operators[15] similarly employed[7,8] in the generalised Nambu representation of the PtM. Explicitly[15]

$$\gamma_0 = \begin{pmatrix} \sigma_0 & 0 \\ 0 & -\sigma_0 \end{pmatrix}, \quad \gamma_5 = \begin{pmatrix} 0 & \sigma_0 \\ \sigma_0 & 0 \end{pmatrix}, \quad \Sigma = \begin{pmatrix} \sigma & 0 \\ 0 & \sigma \end{pmatrix} \tag{2.15}$$

whereas the corresponding Dirac matrices of the Lie-isotopic generalisation are (see, Eqn. (2.3) of ref. 3)

$$\beta = \begin{pmatrix} 0 & \sigma_0 \\ -\sigma_0 & 0 \end{pmatrix}, \qquad \alpha_1 = \begin{pmatrix} 0 & -\sigma_3 \\ -\sigma_3 & 0 \end{pmatrix}, \qquad \alpha_2 = \begin{pmatrix} 0 & \sigma_1 \\ \sigma_1 & 0 \end{pmatrix},$$

$$\alpha_3 = \begin{pmatrix} \sigma_0 & 0 \\ 0 & -\sigma_0 \end{pmatrix}, \tag{2.16}$$

i.e., $A_{03} = \alpha_3$ $A_{31} = -\alpha_1$, e.t.c.

3 NUMERICAL RESULTS

As is well known, the primary interest in the Green's function method is that a knowledge of its Fourier transform can be used to determine the transport and static properties of the system. The present matrix Green's function has the further advantage of ease of the computational algorithm.

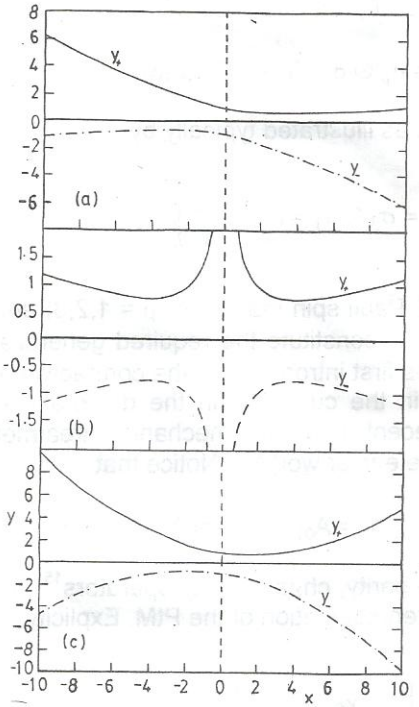

Fig. 1: Approximate normal state excitation energy $y(= E_k/|t|)$ versus level separation $x(= U/|t|, U = \varepsilon_{dk\downarrow} - \varepsilon_{dk\uparrow})$ in the pairing t - model (PtM) of d-p cuprates in the $g_{ak} = \alpha_{sk} = 0$ regime, for: arbitrary U and t (a); |U| >> |t|(b); and |U| << |t|(c).

In this paper, we present, in Figs. 1 and 2, respectively, the excitation energies of the PtM in the normal and SC regimes. Fig. 1 shows the normal state excitation energy $E_k/|t|$ versus level separation $U/|t|$ (where $U = \varepsilon_{dk\downarrow} - \varepsilon_{dk\uparrow}$) in the most convenient approximation $g_{ak=\alpha sk} = 0$, neglecting terms that have higher powers than quadratic in ξ_{ak}, α_{ak} and Δ_{ak} in the expression for the poles of Green's function

$$D \equiv det[i\omega_n - \xi_{ak}, (A_{00} - A_{03}) - \alpha_{ak} A_{33} - \Delta_{ak} A_{13}] = 0. \qquad (3.1)$$

Note that the normal state excitation energies, for arbitrary U and t, are easily found by solving (3.1) in the form[7]

$$E_{k\pm} = -\frac{U}{4} \pm \frac{\sqrt{2}}{4}(U^2 + 8t^2)^{1/2}, \qquad (3.2)$$

and further approximations on (3.2) follow trivially. As indicated in Fig. 1, (a) is for arbitrary U and t; (b), for $|U| >> |t|$, reveals Heisenberg AF spectrum (with $J = -t^2/2U$); and (c), for $|U| << |t|$, reveals a CT spectrum (with possible charge exchange constant, $Q = U^2/16t$ being analogous to the spin exchange constant J). Accordingly, these spectra possibly reveal the two interesting sub-regimes of the normal state of the cuprates in the two-band (d-p) model represented by the PtM in the limit.

Fig.2 represents the SC quasiparticle energies $E_k/|t|$ versus spin energy $\varepsilon_k/|t|$ given, in the $\alpha_{sk} = \frac{1}{4}(\varepsilon_{dk\uparrow} + \varepsilon_{dk\downarrow})$ level symmetry, by

$$E^2_{k\pm} = \varepsilon^2_k + t^2 + \Delta^2_k \pm 2\varepsilon_k t\left(\frac{\varepsilon_K^2}{4} + t^2\right)^{1/2}, \qquad (3.3)$$

for ε_k and t arbitrary (a); $|\varepsilon_k| >> |t|$ (b); and $\varepsilon_k << |t|$ (c). These results are slightly, but not trivially, different from the results plotted in Fig. 5 of ref 7 for a different level symmetry. The JT splitting of the quasiparticle energy is evident but the magnitudes of the JT stabilization energies E_{JT} in Fig. 5 of ref. 7 and Fig. 2, presently, are quite different, as can be observed.

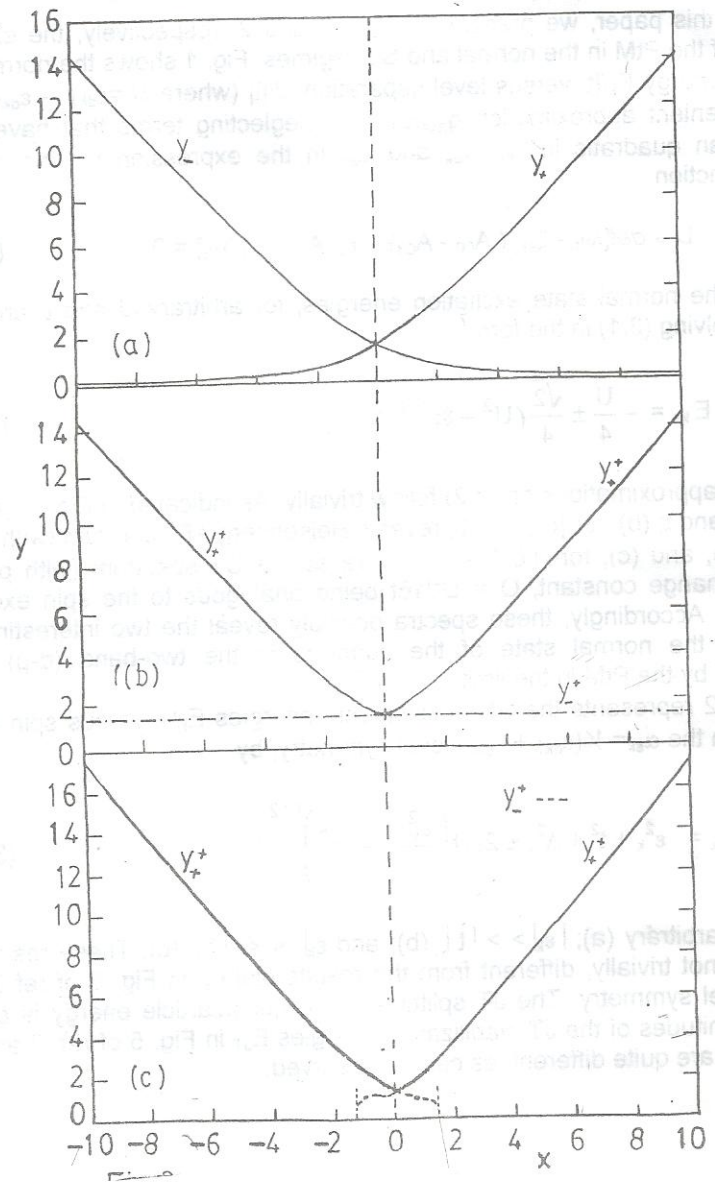

Fig. 2: Superconducting quasiparticle energy $y(= E_k/|t|)$ versus spin energy $x(=\varepsilon_k/|t|)$ in the PtM for d-p cuprates in the $\alpha_{sk} = 1/4(\varepsilon_{dk\uparrow} + \varepsilon_{dk\downarrow})$ level symmetry, for: ε_k and t arbitrary (a); $|\varepsilon_k| >> |t|$(b); and $|\varepsilon_k| << |t|$, showing the Jahn-Teller split in energy.

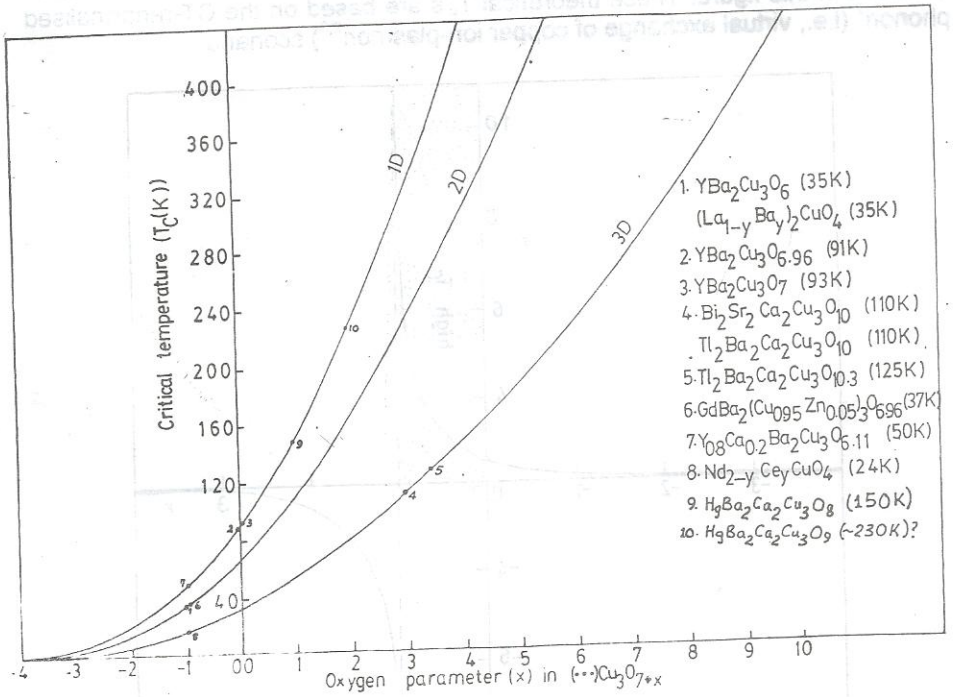

Fig. 3: Superconducting critical temperature (T_C) versus oxygen doping parameter (x) in $(...)Cu_3O_{7+x}$, as by Eqn. (3.4): for one-, two-, and three-dimensional systems, presently including the new monolayer Hg 1:2:2:3 oxide materials. [The realisation of $T_C \sim 97K$ in the d = 1 Hg 1:2:0:1 system, a little higher than the $T_C \sim 93K$ in the d = 1 $YBa_2Cu_3O_7$, point to d = 1 oxide system as the class with the highest promise for easy experimental room-temperature.

In Fig. 3, the SC cririca1 temperature (T_c) is plotted against x (the oxygen doping parameter appearing in (...) $Cu_3 O_{7+x}$) using Eqn. (5.21) of ref. 7:

$$T_c(x) = \Lambda\alpha\left(\frac{n-x}{m}\right) exp\left(-\frac{b'm}{n-x}\right) \qquad (3.4)$$

with the symbols as defined in the reference[7]. This correctly maps the experimental T_c's for a large number of the cuprates, some of which have been indicated in this figure. These theoretical T_c's are based on the CT-renormalised phonon[7] (i.e., virtual exchange of copper ion-plasmon[2,3]) scenario.

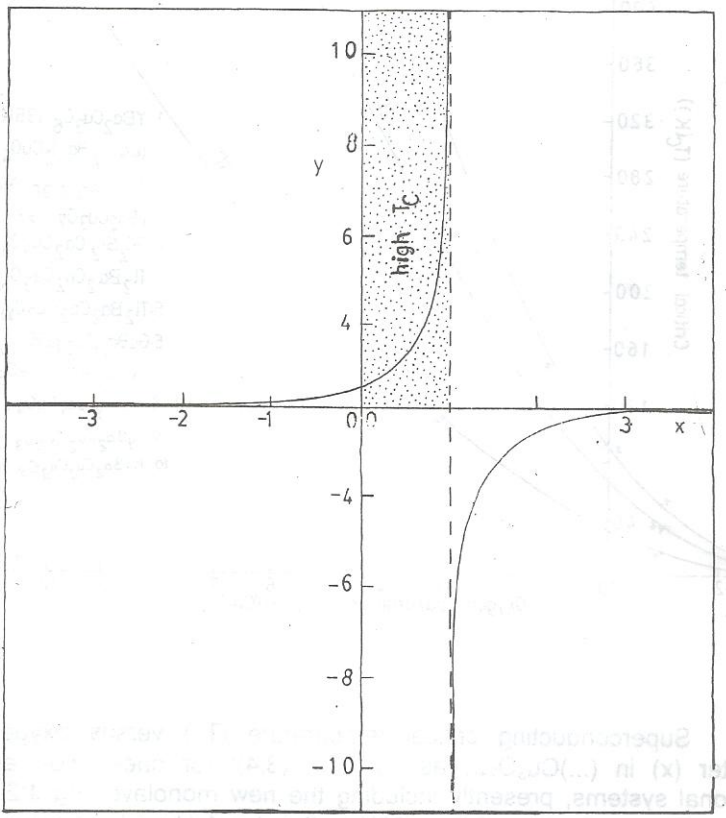

Fig. 4: Variation of the PtM Anderson-type gap $y(=\Delta/\Delta_0)$ of Eqn. (2.2a) at k_F with the hopping matrix ratio $x(=t_{iik}/|2t_{ijk}|$, i ≠ j) showing the most probable region(dotted) for high T_C. [Observe the non-change of sign of the gap for all x < 1 (positive) and x > 1 (negative), respectively, and non-existence of gap nodes for all x except at $x = \pm\infty$].

The variation of the Anderson-type gaps, defined by (2.2a) at k_F, with changes in the hopping matrix ratio, $t_{iik}/|2t_{ijk}|$, $i \neq j$, is shown in Fig. 4. The region of increasing gap with this ratio appears more favourable for the realisation of high T_c than the other regions.

In fig. 5, we have presented the approprimate single spin density of states (DOS) in the SC phase and the α_{sk}= 0 level symmetry, using the definition ($N_s(w) \geq 0$):

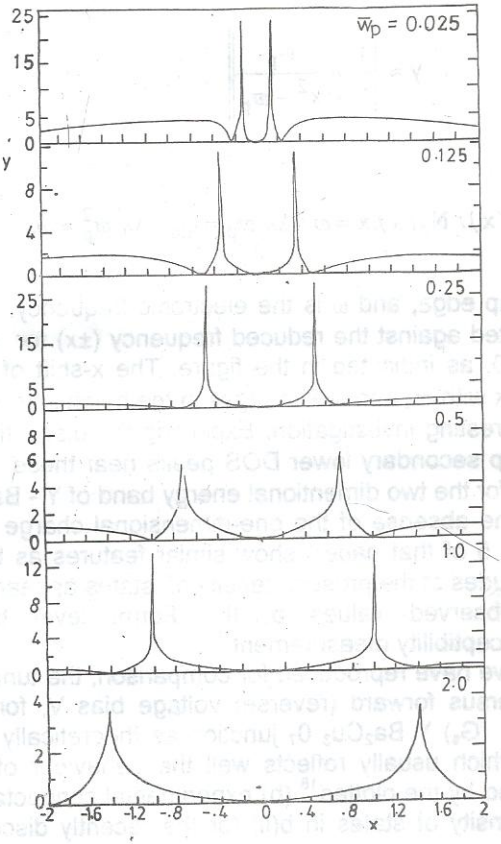

Fig. 5: Approximate reduced single spin density of states $y(= \frac{1}{2}N_s(x)/N_n(x))$ versus reduced electron frequency $x(=\omega/\Delta_0)$ in the PtM, for reduced ion-plasma frequencies $\varpi_p(=\omega_p/\Delta_0)$ as indicated. [Observe the resemblance of these curves to those by the Quantum Monte Carlo simulations by D.J. Scalapino [Results from Numerical Simulations of the 2D Hubbard Model (UCSBTH - 89 – 67 preprint, 1990)] for small on-site repulsion (U ~ 0) in the cuprates].

$$N_s(\omega) = (4\pi)^{-1} \sum_k \mathrm{Tr}\,[\mathrm{Im}G_s(k, i\omega_n \rightarrow \omega + i\delta)], \qquad (3.5)$$

which simplification, in the ion-plasmon ($|\bar{\varepsilon}_k| \leq \hbar\omega_p, \tilde{\varepsilon}_k = \varepsilon_k + t$) scenario, leads to

$$y \approx \left| \frac{1}{x} ln \left| \frac{\varpi_p}{x^2 - \varpi_p} \right| \right| \qquad (3.6)$$

with

$$y = \frac{\pi}{2} N_s(x) / N_n(x), x = \omega / \Delta_0, \varpi_p = \omega_p / \Delta_0, \varpi_p^2 \approx \omega_p,$$

while Δ_0 is the gap edge, and ω is the electronic frequency. The reduced DOS (y) has been plotted against the reduced frequency ($\pm x$) for ϖ_p = 0.025, 0.125, 0.25, 0.5, 1.0, 2.0, as indicated in the figure. The x-shift of the location of the highest DOS peak with ϖ_p and the changes in the heights of these peaks may be objects of an interesting investigation. Expecting the discontinuities at low ω(~ - 2.0) and the sharp secondary lower DOS peaks near these ω values, the D(ω) versus ω curves for the two dimentional energy band of Y - Ba - Cu - 0 by Okabe *et al.*[Ref.14] in the absense of the one-dimensional charge density wave (dot-dash lines of Fig. 5 of that paper) show simlar features as by the present PtM DOS. The magnitudes of the present density of states appear much closer to the experimentally observed values at the Fermi level through the Pauli paramagnetic susceptibility measurement.[16]

In fig. 6, we have reproduced for comparison, the tunneling conductance G_s, and G_s/G_0 versus forward (reverse) voltage bias V, for (a) normal (G_0) - super- conductor (G_s) Y Ba_2Cu_3 0_7 junction as theoretically obtained[17] in BCS framework and which usually reflects well the behaviour of the DOS. Similar trends are revealed by the plotted[18] (b) experimental conductance (i) and (ii) and smeared BCS density of states in b(ii) for the recently discovered single-layer $HgBa_2CuO_{4+\delta}$ cuprate samples with an unsually high T_C ~ 97K.

More detailed considerations of the DOS and the exact consequences of the obtained Anderson-type gap in the PtM are the subject of a separate paper.

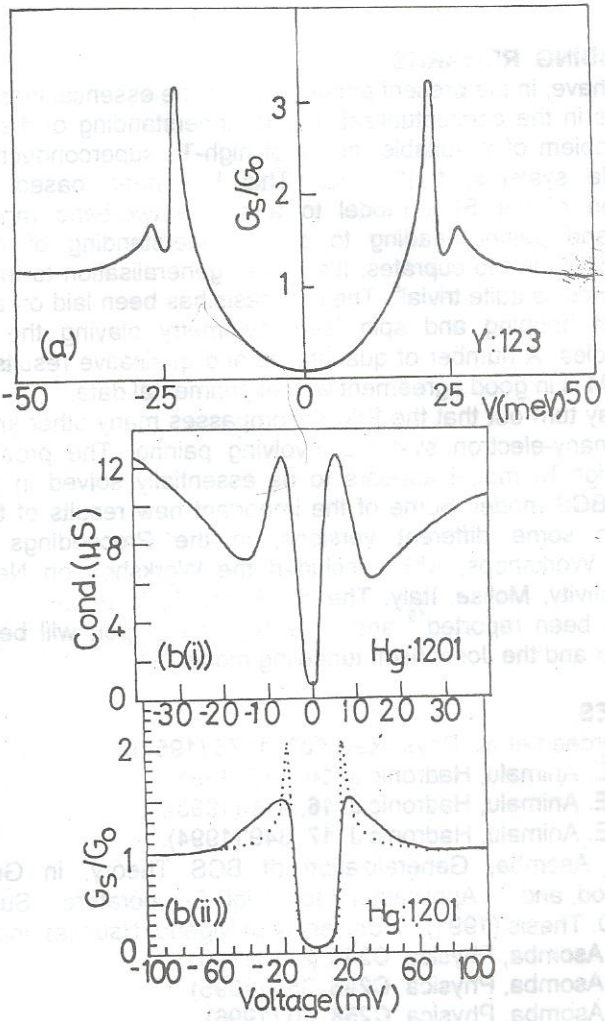

Fig. 6: (Normalised) tunneling conductance $y(=G_s/G_0)$ versus forward (reverse) bias voltage V for:

(a) $YBa_2Cu_3O_7$ [Adapted from Fig. 3 of Ref. 17, copyright 1992, American Institute of Physics];

(b) $HgBa_2CuO_{1+\delta}$: expt. (Solid line), smeared BCS theoretical DOS(ii) (dotted line) [Taken from Figs. 2(f) and 3 of Ref. 18, copyright 1994, American Institute of Physics].

4 CONCLUDING REMARKS

We have, in the present paper, outlined the essential ingredients of some new frontiers in the conceptualization and understanding of the seemingly[3,5,7,8] unsolved problem of a suitable theory of high-T_C superconductivity in the new copper oxide systems, $(...)Cu_mO_{n-x}$. This has been based on the recent generalisation of the BCS model to a simple two-band model of electron correlation and pairing leading to some understanding of magnetism and superconductivity in the cuprates. It's further generalisation to the more realistic multiband model is quite trivial[8]. The emphasis has been laid on electron kinetics with electron hopping and spin level symmetry playing the most decisive conceptual roles. A number of quantitative and qualitative results derived so far within the PtM is in good agreement with experimental data.

It may turn out that the PtM encompasses many other known models of interacting many-electron systems involving pairing. The problem of a valid theoretical high-T_C model appears to us essentially solved in the PtM as an isostandard BCS model. Some of the important new results of this paper were presented in some different versions, in the Proceedings of the I.B.R. International Workshops, which included the Workshop on New Frontiers in Superconductivity, Molise, Italy. The non-Fermi liquid behaviour of the high-T_C systems has been reported[19] and, in a separate paper, will be related to the present paper and the Josephson tunneling model[11,12]

REFERENCES

1. J. Bardeen et al., Phys. Rev. **108**, 1175 (1957).
2. A.O.E. Animalu, Hadronic J. **14**, 457 (1991).
3. A.O.E. Animalu, Hadronic J. **16**, 411 (1993).
4. A.O.E. Animalu, Hadronic J. **17**, 349 (1994).
5. G.C. Asomba, Generalization of BCS Theory, in Green's Funtion Method, and Application to High-Temperature Superconductivity (Ph.D. Thesis (1991), University of Nigeria, Nsukka) unpublished.
6. G.C. Asomba, Physica **C244**, 271 (1995).
7. G.C. Asomba, Physica **C245**, 355 (1995).
8. G.C. Asomba, Physica **C258**, 30 (1996).
9. D. Lurie and S. Cremer, Prog. Theor. Phys. **44**, 300 (1970).
10. F.C. Zhang and T.M. Rice, Phys. Rev. **B37**, 3759 (1988).
11. P.W. Anderson, in: Superconductivity, Proc. of the ICTP Spring College in 1992, P. Butcher and Y. Lu (eds.) (World Scientific, Singapore, 1993).
12. S. Chakravarty et al., Science **261**, 337 (1993).
13. H. Suhl et al., Phys. Rev. Lett. **3**, 552 (1959).
14. Without prejudice to a first introduction of the generalisation $\sigma_\rho \otimes \sigma_\lambda$ of Dirac matrices, GCA adapted this representation $A_{\rho\lambda}$ of our generalised Pauli, Dirac and Gell-Mann matrices from S. Takada (J. Phys. Soc. Jpn. **53**, 1293 (1984).) and the Green's function application from Y. Okabe et

al. (Solid State Comm. **64**, 483 (1987)). Some components of $A_{\rho\lambda}$ were then found to be those Dirac matrices introduced by one of us (AOEA) in Ref. 15. All the earlier uses were in contexts other than multiple-band BCS pairing schemes in the cuprates in the generalised Suhl et al. model of Refs. 5 and 6, or the PtM model (Refs 7 and 8). The non-perturbative, non-diagrammatic, and contractive nature of this approach in handling the multiplicity problems in the cuprates were the most attraction.

15. A.O.E. Animalu, Phys. Rev **B8**, 4420 (1973).
16. Y. Nakazawa et al., Jpn. J. Appl. Phys. **26**, 1796 (1987).
17. R. Lal and S.K. Joshi, Phys. Rev. **B45**, 361 (1992).
18. J. Chen et al., Phys. Rev. **B49**, 3683 (1994).
19. G.C. Asomba, Physica **B266,** 229 (1999).